Formation of Surface-Attached Responsive Gel Layers via Electrochemically Induced Free-Radical Polymerization

Johanna Reuber, Helke Reinhardt, and Diethelm Johannsmann*

Institute of Physical Chemistry, Clausthal University of Technology, Arnold-Sommerfeld-Strasse 4, D-38678 Clausthal-Zellerfeld, Germany

Received December 21, 2005. In Final Form: February 1, 2006

We report on the formation of hydrogel layers on conducting substrates via a simple electrochemical route. Free-radical polymerization is initiated by an electron transfer from the substrate to a redox-active initiator. Gels of the thermally responsive material poly-*N*-isopropylacrylamide (p-NIPAM) with a thickness between 25 and 250 nm were produced and characterized. The gels adhere well to the substrate. They show the characteristic swelling transition at 32 °C. Although the films appear homogeneous in optical microscopy, AFM images reveal a slightly heterogeneous, globular structure. The gels are permeable to small ions as evidenced by electrochemical experiments with gel-covered electrodes.

Introduction

The preparation of hydrogels at solid surfaces is of great practical interest for a number of reasons. Surface-attached gels strongly modify the mechanical and hydrodynamic properties of the surface. Thin films of hydrogels are also extensively used in sensing.[1−3] When functionalized with suitable moieties for molecular recognition, they take up analyte molecules from the bulk in proportion to the concentration of the analyte.[4] The concurrent increase or decrease in the mass of the film can be detected with, for instance, surface plasmon spectroscopy (SPR)[5] or the quartz crystal microbalance (QCM).[6] The gel may also contain electrochemical mediators, allowing for electron transfer between the analyte and the substrate.[7] Further applications of hydrogels at surfaces are in the areas of drug release and tissue engineering.[8] If the release of growth factors for biological cells can be triggered from the substrate (for instance, by application of a voltage), then cell growth can be guided via an in-situ modification of the structure of the gel.

For planar, easily accessible surfaces, a convenient way to produce gel layers consists of depositing a prepolymer by any of the standard methods of film preparation and subsequent cross linking. For complex-shaped surfaces, growing the gels in situ is the preferable way. Also, patterning is easier if the growth process can be controlled locally. Prucker and co-workers have demonstrated an elegant process for gel formation based on a benzophenone moiety attached to the surface via molecular self-assembly.[9] Upon irradiation with UV light, the benzophenone group abstracts a proton from a neighboring polymer chain and forms a covalent bond to this chain. However, this route requires the synthesis of the benzophenone derivative as well as surfaces that are amenable to the self-assembly process.

Another easy way to produce polymer layers on conductive surfaces from polyelectrolyte solutions is electrochemical deposition based on pH gradients.[4] In this case, a voltage is applied to the surface, changing the local proton concentration. The polymers in solution contain charged side groups, which are neutralized in response to the change in pH next to the surface. The neutralization causes a precipitation on the conductive surface.[10]

Here we report on a simple scheme for the production of thin hydrogel layers on conductive surfaces based on an electrochemical initialization. It requires a conductive solvent and a polymer that can be synthesized via free-radical polymerization. In all other respects, the technique is flexible. Also, it is very simple. (Note that this work is not concerned with ordinary electropolymerization of conductive polymers. Waltman, R. J.; Bargon, J. *Can. J. Chem.* **1986**, *64*.) The electrochemically induced polymerization technique has been previously used for acrylic monomers.[11−13] Different methods to initiate polymerization have been demonstrated. Yildiz et al. decomposed potassium persulfate on a silver electrode to initiate the polymerization of acrylamide.[14] Instead of a silver electrode, an aluminum alloy electrode was utilized in the work of Lee and Bell.[15] Yoshizawa et al. used the classical Kolbe electrolysis to produce the initiating radicals.[16] Teng and Mahalingam polymerized acrylonitrile and acrylic acid in sulfuric acid by applying a negative potential.[17] In this case, the initiating species were hydrogen radicals. Collins and Thomas synthesized polyacrylamide in an aqueous solution of zinc chloride.[18] The initiating

* Corresponding author. E-mail: johannsmann@pc.tu-clausthal.de. Phone: + 49-5323-72 3768. Fax: + 49-5323-72 4835.

(1) Feller, J. F.; Guézénoc, H.; Bellégou, H.; Grohens, Y. *Macromol. Symp.* **2005**, *222*, 273.
(2) Blanco-López, M. C.; Gutiérrez-Fernández, S.; Lobo-Castañón, M. J.; Miranda-Ordieres, A. J.; Tuñón- Blanco, P. *Anal. Bioanal. Chem.* **2004**, *378*, 1922.
(3) Herlem, G.; Lakard, B.; Herlem, M.; Fahys, B. *J. Electrochem. Soc.* **2001**, *148*, E435.
(4) Kurzawa, C.; Hengstenberg, A.; Schuhmann, W. *Anal. Chem.* **2002**, *74*, 355.
(5) Matsui, J.; Akamatsu, K.; Hara, N.; Miyoshi, D.; Nawafune, H.; Tamaki, K.; Sugimoto, N. *Anal. Chem.* **2005**, *77*, 4282.
(6) Nakanishi, K.; Muguruma, H.; Karube, I. *Anal. Chem.* **1996**, *68*, 1695.
(7) Schuhmann, W.; Kranz, C.; Huber, J.; Wohlschläger, H. *Synth. Met.* **1993**, *61*, 31.
(8) Kikuchi, A.; Okano, T. *J. Controlled Release* **2005**, *101*, 69.
(9) Prucker, O.; Naumann, C. A.; Rühe, J.; Knoll, W.; Frank, C. W. *J. Am. Chem. Soc.* **1999**, *121*, 8766.
(10) Beck, F. *Electrochim. Acta* **1988**, *33*, 839.
(11) Baute, N.; Jérôme, C.; Martinot, L.; Mertens, M.; Geskin, V. M.; Lazzaroni, R.; Brédas, J. L.; Jérôme, R. *Eur. J. Inorg. Chem.* **2001**, 1097.
(12) Yamazaki, N. *Adv.* Polym. *Sci.* **1969**, *6*, 377.
(13) Lee, C. S.; Bell, J. P. *J. Mater.* Sci. **1995**, *30*, 3827.
(14) Yildiz, G.; Çatalgil-Giz, H.; Kadirgan, F. *J. Appl. Electrochem.* **2000**, *30*, 71.
(15) Lee, C. S.; Bell, J. P. *J. Mater. Sci.* **1995**, *30*, 3827.
(16) Ogumi, Z.; Tari, I.; Takehara, Z.; Yoshizawa, S. *Bull. Chem. Soc. Jpn.* **1974**, *8*, 1843.
(17) Teng, F. S.; Mahalingam, R. *J. Appl. Polym. Sci.* **1979**, *23*, 101.

10.1021/la053454o CCC: $33.50
Published on Web 03/07/2006

species was believed to be a complex between the zinc cations and the monomer. Speiser and co-workers investigated the polymerization of 4-ethenyl[2_2]paracyclophane in organic solvents.[19] The initiating species was a radical cation arising from anodic oxidation of the monomer. Palacin et al. performed electrografting in inorganic solvents.[20] The polymers grow from a radical adsorbed on the conductive surface.

This work focuses on the thermally responsive material poly-*N*-isopropylacrylamide (p-NIPAM). Interest in the p-NIPAM system stems from the fact that it has a fully reversible lower critical solution temperature (LCST) in water at around 32 °C.[21] Because this temperature lies between room temperature and body temperature, p-NIPAM is of interest in biological applications. Above the critical temperature, the polymer phase separates from solution, whereas below it the polymer is soluble. The lower critical solution temperature is a result of the entropy gain upon the dehydration of the amide moieties with increasing temperature and can be affected by additives such as salt,[22,23] alcohol,[24] and surfactants[25] and by the variation of the solution pH.[26] In recent years, different methods of grafting p-NIPAM onto solid surfaces were reported, including atom-transfer radical polymerization,[27] plasma polymerization,[28] growth from self-assembled monolayers (SAMs) composed of azo initiators ("grafting from"),[29,30] photo cross linking of a prepolymer,[31] grafting of thiol-terminated p-NIPAM to gold substrates ("grafting to"),[32] and electron beam irradiation.[33] When attached to a solid surface, the p-NIPAM layer swells and deswells with temperature. In this way, one can tune the thickness of the layer and its softness.[34] Gels of p-NIPAM show temperature-induced shape transformations that make them useful as sensors and actuators.[35] Above the LCST, the surface of the gel is hydrophobic (that is, collapsed), whereas it is hydrophilic (that is, expanded) below. p-NIPAM layers have been used as microvalves in microfluidic systems[36] as well as for thermally controlled drug release[37] and for tissue engineering.[8]

Experimental Section

Sample Preparation. A sketch of the setup is shown in Figure 1. The polymer layers grow on the front electrode of an electrochemical quartz crystal microbalance (EQCM),[38] where the latter allows for in-situ monitoring of the film growth. The shifts in frequency, Δf, and half-band-half-width, $\Delta\Gamma$, ("bandwidth" for short) were determined by impedance analysis. Resonance curves were fitted to the admittance spectra as determined with a network analyzer (E5100A, Agilent). The frequency shift, Δf, was converted to a film thickness, d_S, by means of the Sauerbrey equation

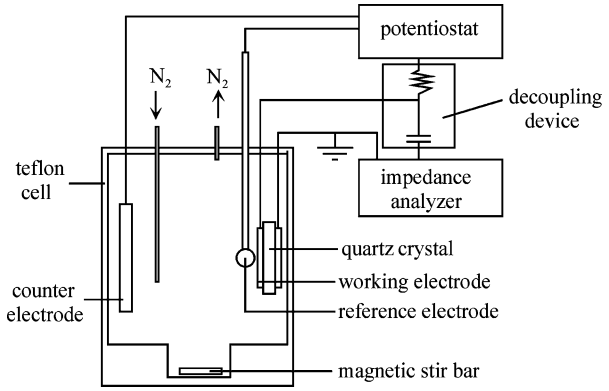

Figure 1. Setup of the electrochemical quartz crystal microbalance for the electrochemically induced polymerization of NIPAM on the front electrode of a quartz crystal resonator.

$$\Delta f = -\frac{2nf_f^2}{Z_q} m_S = -\frac{2nf_f^2}{Z_q} \rho_f d_S \qquad (1)$$

where Δf is the frequency shift, f_f is the frequency of the fundamental, n is the overtone order, $Z_q = 8.8 \times 10^6$ kg m^{-2} s^{-1} is the acoustic impedance of AT-cut quartz, m_S is the mass per unit area of the film, $\rho_f \approx 1$ g/cm^3 is the density of the film, and d_S is the film thickness in the Sauerbrey sense, which is also called the "Sauerbrey thickness". It is known that the Sauerbrey relation often does not yield the true mass when applied to films in liquids. Both m_S and d_S are effective quantities, representing the apparent mass as calculated by eq 1.

The polymerization was carried out under potentiostatic control (PGU 10V-1A IMP, Jaissle, Germany) in a three-electrode configuration using a home-built Teflon cell with a platinum plate as the counter electrode, a saturated calomel reference electrode (SCE, Sensortechnik Meinsberg, Germany), and the gold electrode of a 5 MHz AT-cut quartz crystal resonator (Maxtek, Santa Fe Springs, CA) as the working electrode.

Before the polymerization, the front electrode of the quartz crystal resonator was electrochemically cleaned in 1 M sulfuric acid. For this purpose, a triangular potential wave from 0 to −1 V was applied until the cyclic voltammograms reached a stationary state (usually 2 h or more). In preparation for the polymerization process, a solution of 0.4 mol/L potassium sulfate (Riedel de Haën) in distilled water was prepared and sonicated for at least 30 min to remove dissolved gases. The monomer (*N*-isopropylacrylamide, NIPAM, Acros, 0.3 mol/L), the cross linking agent (*N*,*N*′-methylendiacrylamide, BIS, Merck, concentration varying between 1 and 10 mmol/L), and the initiator (potassium persulfate, Merck, 10 mmol/L) were added. The solution was injected into the cell and bubbled with nitrogen. Before and after each measurement, a cyclic voltammogram (CV, −1 to 0.2 V, 100 mV/s) was acquired. In principle, the negative potential applied during the CV taken before each polymerization should already induce some polymerization. However, on the basis of the frequency shift of the QCM, we conclude that the thickness of this film is below our detection limit. The polymerization was initiated by applying a voltage of −0.8 V versus the saturated calomel electrode (SCE). The polymerization time varied between 10 s and 50 min. For selected cases, we also performed experiments with voltages of −0.6 and −0.7 V.

IR Spectroscopy. The quartz resonators coated with the hydrogel films were dried with nitrogen until the frequency reached a stationary state. The FTIR spectrometer (Bruker IFS, 66v/S) contained a home-built adapter for measurements in reflection with p-polarized light. The angle of incidence was 78°. Figure 2 displays spectra based on averages of 512 interferograms.

(18) Collins, G. L.; Thomas, N. W *J. Polym. Sci., Polym. Ed.* **1977**, *15*, 1819.
(19) Gollas, B.; Hesse, I.; Lotz, R.; Pasch, H.; Speiser, B.; Zagos, I. *Liebigs Ann. Recl.* **1997**, 2255.
(20) Palacin, S.; Bureau, C.; Charlier, J.; Deniau, G.; Mouanda, B.; Viel, P. *ChemPhysChem* **2004**, *5*, 1468.
(21) Schild, H. G. *Prog. Polym. Sci.* **1992**, *17*, 163.
(22) Zhang, Y.; Furyk, S.; Bergbreiter, D. E.; Cremer, P. S. *J. Am. Chem. Soc.* **2005**, *127*, 14505.
(23) Freitag, R.; Garret-Flaudy, F. *Langmuir* **2002**, *18*, 3434.
(24) Liu, G.; Zhang, G. *Langmuir* **2005**, *21*, 2086.
(25) Lynch, I.; Sjöström, J.; Piculell, L. *J. Phys. Chem. B* **2005**, *109*, 4252.
(26) Graziano, G. *Int. J. Biol. Macromol.* **2000**, *27*, 89.
(27) Balamurugan, S.; Mendez, S.; Balamurugan, S. S.; O'Brian, M. J.; López, G. P. *Langmuir* **2003**, *19*, 2545.
(28) Pan, Y. V.; Wesley, R. A.; Luginbuhl, R.; Denton, D. D.; Ratner, B. D. *Biomacromolecules* **2001**, *2*, 32.
(29) Tovar, G.; Paul, S.; Knoll, W.; Prucker, O.; Rühe, J. *Supramol. Sci.* **1995**, *2*, 89.
(30) Prucker, O.; Müller, K.; Rühe, J. *Mater. Res. Soc. Symp.* **2000**, 62.
(31) Kuckling, D.; Tang, M.; Frank, C. W. *Macromolecules* **2002**, *35*, 6377.
(32) Cho, E. C.; Kim, Y. D.; Cho, K. *Polymer* **2004**, *45*, 3195.
(33) Yamada, N.; Okano, T.; Sakai, H.; Karikusa, F.; Sawasaki, Y.; Sakurai, Y. *Makromol. Chem. Rapid Commun.* **1990**, *11*, 571.
(34) Arndt, K. F.; Kuckling, D.; Richter, A. *Polym. Adv. Technol.* **2000**, *11*, 496.
(35) Kuckling, D.; Vo, C. D.; Wohlrab, S. E. *Langmuir* **2002**, *18*, 4263.
(36) Harmon, M. E.; Tang, M.; Frank, C. W. *Polymer* **2003**, *44*, 4547.
(37) Bae, Y. H.; Okano, T.; Kim, S. W. *Pharm. Res.* **1991**, *8*, 624.
(38) Buttry, D. A.; Ward, M. D. *Chem. Rev.* **1992**, *92*, 1355.

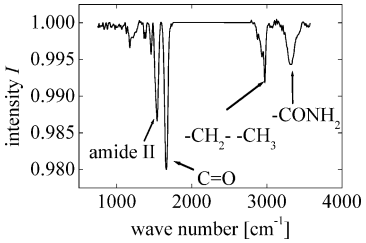

Figure 2. FTIR spectrum of a p-NIPAM layer with a thickness of 60 nm in the collapsed state. The spectrum was taken in reflection mode using p-polarized light at an angle of incidence between 75 and 89°. The spectrum shows all of the bands expected for p-NIPAM.

Atomic Force Microscopy. The microscopic structure of the gel was investigated with an atomic force microscope (AFM). Gels of 33 nm thickness (in the collapsed state) were analyzed in water at room temperature. The AFM (BioScope AFM, Veeco Metrology Group) was operated in tapping mode. Films with a thickness of 75 nm were imaged in air, also using the AFM (extended multimode, NanoScope IIIa controller, Veeco/Digital Instruments) in tapping mode.

Swelling Behavior. To check for the swelling transition at 32 °C characteristic of p-NIPAM gels, the quartz crystal was mounted in a home-built, temperature-controlled liquid cell. The long-time stability of the cell is about ±0.2 °C. The temperature was linearly cycled between 24 and 43 °C in distilled water at a ramp rate of 0.08 °C/min.

Cyclic Voltammetry with Potassium Ferricyanide. To investigate the transport characteristics of the gel layer, the sample was exposed to a solution of potassium ferricyanide ($K_3[Fe(CN)_6]$, 5 mmol/L in 0.4 mol/L aqueous potassium sulfate), and cyclic voltammograms were acquired as a function of the dwell time. A triangular potential wave from −0.4 to 0.6 V with 100 mV/s was applied.

Results and Discussion

The shifts in frequency, Δf, and bandwidth, $\Delta\Gamma$, the current density, j, and the Sauerbrey thickness, d_S, during a typical polymerization run are shown in Figure 3. For this particular experiment, the initiator concentration and the cross-linker concentration were 10 and 3 mmol/L, respectively. The polymerization was initiated by applying a potential of −0.8 V versus SCE. The total polymerization time was 10 min. The fact that the Sauerbrey mass is the same on the different harmonics indicates that the film's rigidity greatly exceeds the rigidity of water. For such a situation, elastic contributions to the Sauerbrey thickness may be ignored.[39] The same conclusion is reached from the fact that the increase in bandwidth is small (Figure 3b). When elastic corrections are strong, one usually also observes a strong increase in bandwidth. This is not the case. We do not attribute a special significance to the shifts in bandwidth apart from the fact that the shift is small. Note that the Sauerbrey thickness does include trapped water even in the absence of elastic corrections. The fact that elastic contributions are absent does not imply that the film is solvent-free. The issues of trapped mass and elastic contributions are separate.[40]

The Sauerbrey thickness as determined immediately after polymerization is different from the thickness determined after drying (Table 1). The final (wet) thickness reached after 10 min of polymerization is about 100 nm. The ratio of wet and dry thickness (swelling ratio) decreases with polymerization time. A typical swelling ratio obtained after 30 s of polymerization is around 4, whereas a polymerization time of 10 min leads to a swelling ratio of around 1.3. Clearly, there is a densification during polymerization. The swelling ratio of the films substantially *increased* when replacing the electrolyte with pure water after the polymerization. As demonstrated in Figure 4, the presence of 0.4 M K_2SO_4 induces a collapse of p-NIPAM. Presumably, precipitation during polymerization increases the efficiency of film formation and adhesion to the substrate because it inhibits the diffusion of newly formed chains away from the substrate. Note, however, that the film quality was unsatisfactory when the cross linker had been entirely eliminated. Cross linking is needed.

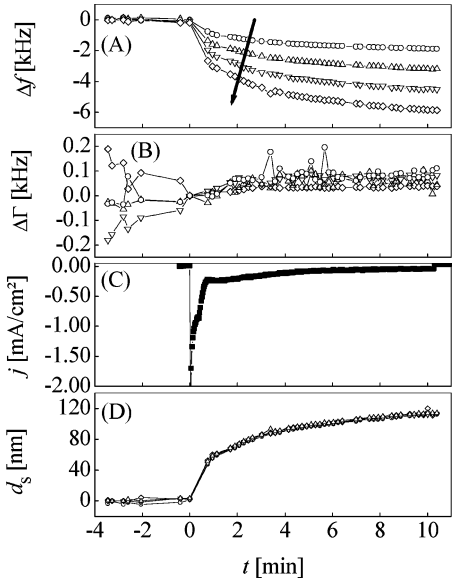

Figure 3. Shift in frequency, Δf (A), shift in half-band-half-width, $\Delta\Gamma$ (B), current density j (C), and Sauerbrey thickness, d_S (D) during a polymerization process. The overtones used were 15, 25, 35, and 45 MHz. The arrow indicates increasing overtone order. The polymerization was initiated by applying a potential of −0.8 V. The film grows on the front electrode of the quartz crystal, causing the negative frequency shift. As indicated by both the current density and the frequency shift, the polymerization proceeds quickly during the first minute and slows down afterward. The Sauerbrey thickness, d_S, was calculated from the frequency shift by means of the Sauerbrey equation (eq 1).

Table 1. Influence of the Preparation Parameters on the Thickness, the Speed of Growth, and the Swelling Ratio[a]

	d_S (nm)	speed of growth (nm/min)	wet thickness/ dry thickness
	pH		
0.4 M K_2SO_4 + 0.025 M H_2SO_4, pH 2.6	113	42	
0.4 M K_2SO_4, pH 4.7	141	37	1.3
	Cross-Linker Concentration		
1 mol % BIS	33		3.75
5 mol % BIS	51		3.64
10 mol % BIS	56		3.62
	Polymerization Time		
10 s	33		3.75
6 min	73		1.33
50 min	82		1.42
	Voltage		
−0.6 V	25	2	1.4
−0.7 V	95	12	1.6
−0.8 V	118	19	1.4

[a] The concentrations of monomer and supporting electrolyte were maintained constant at 0.3 and 0.4 mol/L, respectively. The standard conditions are given by a polymerization time of 10 min, a pH of 4.7, a cross-linker concentration of 3 mmol/L, and a voltage of −0.8 V. Standard conditions apply whenever the respective parameter is not varied as stated in the first column.

(39) Johannsmann, D. *J. Appl. Phys.* **2001**, *89*, 6356.
(40) Johannsmann, D. *Macromol. Chem. Phys.* **1999**, *200*, 501.

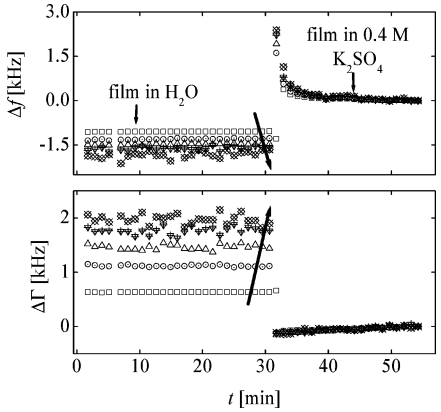

Figure 4. Shifts in frequency, Δf, (top) and bandwidth, $\Delta\Gamma$, (bottom) of a film in water and in 0.4 M K_2SO_4. The overtones used were 15, 25, 35, 45, and 55 MHz, where the arrows indicate increasing overtone order. The p-NIPAM film is fully expanded in distilled water, which results in strong elastic contributions to Δf and $\Delta\Gamma$. When exchanging the water with 0.4 M K_2SO_4, the film collapses. This proves that the p-NIPAM layer grows in the collapsed state during the polymerization process.

After a period of 3 days, precipitated bulk polymer was found in the bulk of the electrochemical cell, as well. As expected, some of the chains leave the surface.

The film growth slows down with time, which presumably is caused by the decreased accessibility of the surface with increasing coverage. This interpretation is corroborated by the decrease in current with time. The same conclusion is reached by two other observations: First, cyclic voltammograms taken before and after polymerization (Figure 7) show that the peak resulting from the decomposition of potassium persulfate decreases during polymerization. Second, cyclic voltammograms taken after polymerization in the presence of potassium ferricyanide show a greatly impeded diffusion of ions through the hydrogel film (Figure 9).

Integration of the current over time yields a total charge in the range of -0.01 C/cm^2. The comparison of charge and monomer conversion shows that the efficiency with which an electron leaving the cathode produces surface-adsorbed polymer is rather low. Assuming a swelling ratio of 3.7, a wet film thickness of 100 nm, a density of 1 g/cm^3, and a molecular weight of the repeat unit of 112 g/mol, we arrive at a total amount of converted and surface-adsorbed monomer of 10^{-8} mol/cm^2 or equivalently 10^{-6} mol/C. Note that some polymer leaves the surface and diffuses into the bulk (as evidenced by the presence of precipitated polymer at the bottom of the chamber after long polymerization times). These chains are not included in the calculation above. A current efficiency in percent cannot be calculated because this number would concern the number of initiation events. The experimentally accessible parameter is the film thickness (including trapped water); the conversion to the number of initiation events would require a few unknown parameters (such the ratio of the propagation rate and the termination rate).

Presumably, some of the radicals produced at the electrode are inactivated before the polymerization starts. A small radical escape efficiency is suggested in ref 41. These authors investigated the redox behavior of persulfate ions on gold electrodes in an aqueous medium. They propose that the ions are reduced at negative potentials according to

$$S_2O_8^{2-} + e^- \rightarrow\rightarrow SO_4^{\bullet -} + SO_4^{2-} \quad (2)$$

$$SO_4^{\bullet -} + e^- \rightarrow SO_4^{2-} \quad (3)$$

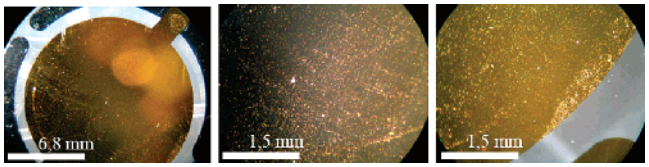

Figure 5. Optical micrographs of a crystal covered with a gel layer produced under standard conditions. The films appeared to be very homogeneous. Inhomogeneities were due to scratches and defects in the gold substrate.

In reaction 2, the initiating sulfate radical anions are produced. In some cases, this first step is followed by the fast uptake of a second electron (eq 3). The radical anions that escape induce a polymerization as shown in reactions 4 and 5:

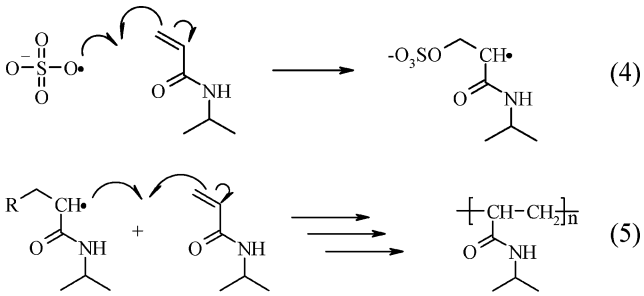

Figure 2 shows IR spectra of the films on the working electrode. They prove that surface-bound p-NIPAM was indeed obtained.

Figure 5 shows optical micrographs of the film. The film covers the entire electrode and is optically homogeneous. In particular, these films show no indications of hydrogen bubbles. Hydrogen bubbles do occur when the reaction is carried out at more negative potentials or lower pH. Hydrogen evolution is a process that competes with initiation by a redox process. Figure 6 shows AFM micrographs of films in water and in air. The films that appear perfectly flat in optical microscopy have a globular structure on the nanoscopic scale. We can only speculate about the reason for the heterogeneity. One explanation builds on the observation that the electrolyte introduces a collapse of the film. Because the solubility in such a situation depends on molecular weight, one may hypothesize that the globules in Figure 6 correspond to chains or microgels that have reached the critical size for collapse. Another explanation is based on the fact that the probability that a freshly formed chain escapes into the bulk decreases if the respective chain is formed inside a gel. Once physisorbed polymer chains have formed at a certain spot, these chains will trap further chains created at the same spot and thereby increase the size of this globule. Chains that form between such globules desorb much more easily.

The adhesion of the films to the substrates appeared to be good. The quartz plates covered with the films were easy to handle. Softly touching the films with tweezers did not leave scratches. The films did not desorb when stored in water or salt solution, even after several weeks. Presumably, adhesion is improved by the fact that the gel is formed in situ and therefore perfectly matches the substrate in shape.

Cyclic voltammograms acquired before and after the polymerization are shown in Figure 7. The large peak at about -0.9 V results from the decomposition of the initiator. After the polymerization, this peak has greatly decreased, indicating that the diffusion of the initiator to the electrode surface is impeded by the polymer layer.

(41) Samec, Z.; Doblhofer, K. *J. Electroanal.* Chem. **1994**, *367*, 141.

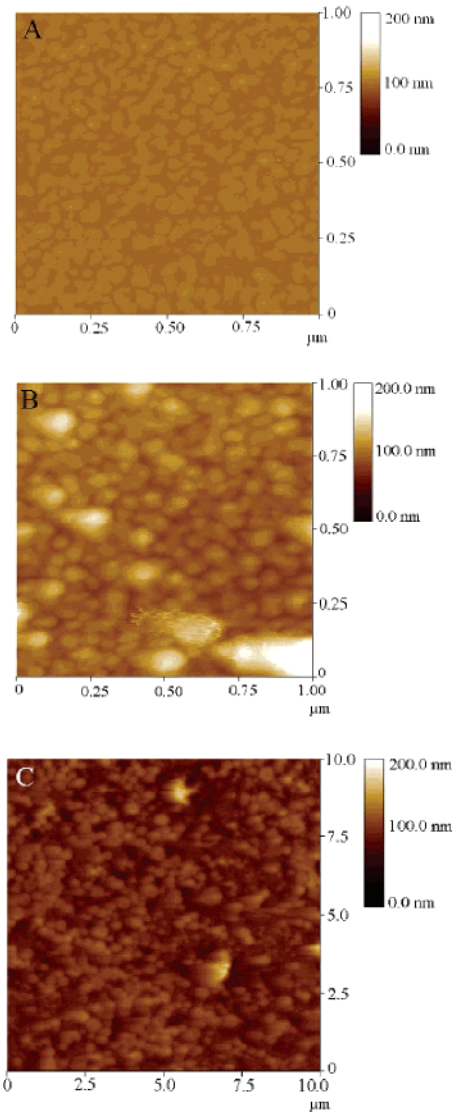

Figure 6. AFM micrographs of an electrochemically cleaned gold electrode (A), a p-NIPAM film with a thickness of 33 nm at room temperature in water (B), and a film with a thickness of 75 nm in air (C). The films that appeared homogeneous in optical microscopy were quite heterogeneous on the nanoscopic scale. The reasons for such a globular structure remained unclear.

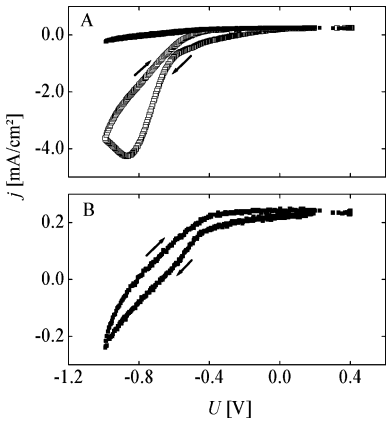

Figure 7. Cyclic voltammograms taken with a sweep rate of 100 mV/s in the reaction mixture before (□) and after (■) 10 min of polymerization (A). Panel B shows an enlarged plot of the CV taken after the polymerization. The peak in panel A at around −0.9 V resulted from the reduction of $K_2S_2O_8$ as proven by reference measurements. This peak disappeared after the polymerization.

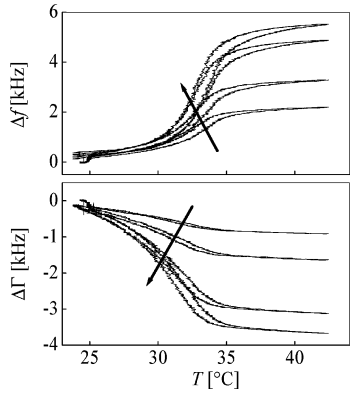

Figure 8. Ramping the temperature of the gel, one finds the characteristic swelling transition of p-NIPAM gels, caused by the LCST behavior. The swelling transition was detected by means of the quartz crystal microbalance. The expulsion of water from the network caused the mass of the film to decrease and the frequency of the quartz crystal to increase. The harmonics used were at 15, 25, 45, and 55 MHz. The arrows indicate increasing overtone order.

The influence of pH, cross-linker concentration, polymerization time, and applied voltage on the film thickness, polymerization kinetics, and swelling ratio is summarized in Table 1. The observed trends can be summarized as follows:

−The efficiency of film growth increases with increasing pH because hydrogen evolution, which is a competing process, speeds up with proton concentration.

−The final film thickness increases with cross-linker concentration. Presumably, the cross linker prevents the desorption of newly formed chains from the polymer layer. Contrary to intuition, the cross-linker concentration hardly affected the swelling ratio of the film. However, entirely eliminating the cross linker resulted in poor reproducibility of the data as well as poor adhesion of the films to the substrate.

−The swellability of the film strongly decreases with the time of polymerization, indicative of an increase in the polymer volume fraction. The QCM cannot in situ determine the solvent fraction of a film. The polymer volume fraction was inferred from the comparison of wet and dry thicknesses after the polymerization process was complete. The change in polymer volume fraction is very fast in the first few seconds of polymerization. The dependence of thickness and swellability on time levels off after about 30 s.

−There is a very strong increase in the speed of growth when shifting the electrode potential to more negative values. However, hydrogen evolution deteriorates the film quality when the potential approaches −1 V. A voltage of −0.8 V proved to be a good compromise.

Figure 8 shows the frequency and bandwidth shift of the film-covered quartz in pure water as a function of temperature. The films show the familiar swelling transition of p-NIPAM gels at 32 °C. The fact that this swelling transition is found at the bulk lower critical solution temperature (LCST) proves, even more stringently than IR spectroscopy, that p-NIPAM has actually been formed at the surface. The temperature scan is an easy and convenient check for successful polymerization. In some cases, we have also found transition temperatures that are different from 32 °C. This aspect needs further investigation. There are a number of reasons (density, degree of cross linking, flexibility of the chains, etc.) why the properties of the surface-bound gel might differ from the properties of the bulk material.

Figure 9 addresses the transport behavior. Generally speaking, hydrogels should be permeable to ions, which makes them

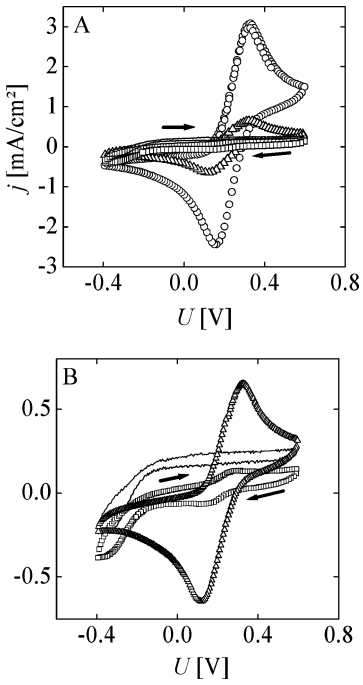

Figure 9. Cyclic voltammograms (CVs) of $K_3[Fe(CN)_6]$ (5 mmol/L in 0.4 mol/L aqueous potassium sulfate). (A) □, 102 nm polymer layer, immediately after the addition of $K_3[Fe(CN)_6]$; △, 102 nm polymer layer, 20 min after the addition of $K_3[Fe(CN)_6]$; −, reference experiment, 102 nm polymer layer in the absence of $K_3[Fe(CN)_6]$; ○, bare crystal. Panel B shows an enlarged plot of the experiments with the polymer layer. The CVs allow for an estimation of the diffusion constants of the ions inside the collapsed p-NIPAM film. The first cycles show no indication of the typical peaks of $K_3[Fe(CN)_6]$. After two cycles, peaks start to appear. After a dwell time of 20 min, a CV is observed, which is stationary in time. This proves that the diffusion of ions to the electrode surface is impeded by the collapsed hydrogel film.

attractive as matrixes for electrochemical mediators or ion-selective membranes. We performed experiments allowing for an estimate of the permeability by acquiring cyclic voltammograms from a potassium ferricyanide solution ($K_3[Fe(CN)_6]$ in 0.4 mol/L aqueous potassium sulfate). The fact that the peak separation is above the theoretical value for a reversible redox pair under diffusion control (58/n mV) points to a barrier, the nature of which is unclear. Note that the film is collapsed in this solution. As the Figure shows, the diffusion of ions through the gel layer takes some time. Immediately after the addition of potassium ferricyanide to the solution, the CV curve (data not shown) is essentially the same as for the pure electrolyte (−). After four cycles (□), a small characteristic redox peak is found. After a dwell time of about 20 min (△), a stationary state is reached. The peak height is about one-third of the peak height found in the absence of the polymer layer (○). If the speed of permeation is a prime concern, then thinner films with larger water content can be employed. With a film thickness of about 100 nm, an equilibration time of 1 min converts to a diffusion coefficient in the range of 10^{-15} m^2/s. Slow diffusion in the late stages of polymerization is also evident from the decrease in the speed of film growth.

Conclusions

Electrochemically induced polymerization is an easy and versatile route for the production of surface-attached hydrogel layers. IR spectroscopy and the occurrence of the swelling transition prove that the target structure, p-NIPAM, has been formed. The surface-adsorbed polymer films may find applications as materials for tissue engineering, for sensing, and for microvalves or actuators in microfluidic devices.

Acknowledgment. We thank W. Oppermann for numerous stimulating and helpful discussions. The AFM images were acquired by F. Dupont in the group of P. Vermette, Université de Sherbrooke, and by I. Reviakine, Clausthal University of Technology. The FTIR measurements were made by J. Vogel in the group of W. Daum, Clausthal University of Technology.

LA053454O